Available online at www.sciencedirect.com
SCIENCE DIRECT®
Physics Letters B 612 (2005) 165–172
PHYSICS LETTERS B
www.elsevier.com/locate/physletb

Polarized proton scattering on ^{58}Ni at small momentum transfer: A test of the microscopic optical model and effective interactions ☆

F. Hofmann [a,1], C. Bäumer [b], A.M. van den Berg [c], D. Frekers [b], V.M. Hannen [c,2], M.N. Harakeh [c], M.A. de Huu [c,3], Y. Kalmykov [a], P. von Neumann-Cosel [a], V.Yu. Ponomarev [a,4], S. Rakers [b], B. Reitz [a,5], A. Richter [a], A. Shevchenko [a], K. Schweda [a,6], J. Wambach [a], H.J. Wörtche [c]

[a] *Institut für Kernphysik, Technische Universität Darmstadt, 64289 Darmstadt, Germany*
[b] *Institut für Kernphysik, Universität Münster, 48149 Münster, Germany*
[c] *Kernfysich Versneller Instituut, 9747 AA Groningen, The Netherlands*

Received 8 November 2004; received in revised form 16 February 2005; accepted 7 March 2005

Available online 17 March 2005

Editor: V. Metag

Abstract

The reaction ^{58}Ni$(\vec{p}, \vec{p}')$ has been studied at small scattering angles and an incident beam energy of 172 MeV. We extract cross sections and analyzing powers for elastic scattering and transitions to vibrational states at low excitation energies. The data are compared to DWBA98 calculations using different widely used effective projectile–target interactions and the quasiparticle–phonon model including complex configurations for the nuclear structure input. The comparison with the experimental data reveals surprising discrepancies for elastic scattering observables at forward angles, whereas the prominent inelastic transitions to low-lying states are well described.

☆ Work supported by the DFG under contract SFB 634, Land Nordrhein-Westfalen, the EU under contract TMR-LSF ERBIMGECT980125 and by the Nederlandse Organisatie voor Wetenschappelijk Onderzoek as part of the research program of the Stichting FOM.
E-mail address: vnc@ikp.tu-darmstadt.de (P. von Neumann-Cosel).
[1] Present address: Kassenärztliche Vereinigung Bayerns, 81925 München, Germany.
[2] Present address: II. Physikalisches Institut, Universität Giessen, 33592 Giessen, Germany.
[3] Present address: Contrinex SA, 1762 Givisiez, Switzerland.
[4] Permanent address: Bogoliubov Laboratory for Theoretical Physics, Joint Institute for Nuclear Research, Dubna, Russia.
[5] Present address: Thomas Jefferson National Accelerator Facility, Newport News, VA 23606, USA.
[6] Present address: Lawrence Berkeley National Laboratory, Berkeley, CA 94720, USA.

0370-2693/$ – see front matter
doi:10.1016/j.physletb.2005.03.020

PACS: 25.40.Cm; 25.40.Ep; 24.10.-i; 27.40.+z

Keywords: REACTION ^{58}Ni($\vec{p}, \vec{p}'$) at $E_0 = 172$ MeV; measured $d\sigma/d\Omega$ and A_n, elastic and inelastic scattering; DWBA, effective NN interactions, quasiparticle–phonon model.

The microscopic description of cross sections and analyzing powers in hadron scattering is a long-standing problem. Difficulties arise because of the complexity of the projectile–target interaction on the one hand and of the nuclear response to an external probe on the other hand. However, as Amos et al. [1] pointed out in a recent review "*the microscopic optical model has progressed to a stage where a long held goal may be achieved, namely to predict cross sections and spin observables for nucleon–nucleus (NA) scattering with confidence that they are correct to a high degree*". The present work contributes to a critical examination of this conclusion by a measurement of transverse polarized proton scattering on ^{58}Ni. Emphasis is put on data at small scattering angles, i.e., small momentum transfer, where experimental information is generally scarce.

Besides the genuine interest to approach a solution of the complex hadron scattering problem, a high-quality optical model description, in particular at small angles, is mandatory for the extraction of nuclear structure information. As an example, recent experimental and theoretical efforts have focused on a systematic understanding of isovector spin–flip modes such as the Gamow–Teller (GT) resonance, characterized by a transferred angular momentum $\Delta L = 0$, and the spin-dipole (SD) resonance with $\Delta L = 1$. This interest is partly driven by new experimental developments permitting the study of charge-exchange reactions with high resolution (see, e.g., [2,3] and references therein), providing access to different isospin components of these resonances. An extraction of the corresponding modes from proton scattering would provide a complete isospin set [4], which in turn would serve as a unique testing ground for microscopic calculations. Furthermore, the GT and SD resonances also have important astrophysical implications providing information on the analog weak decay modes [5]. The GT_0 response to transitions with ground state isospin $T = T_0$, which could be extracted from (p, p') data, allows to model neutral-current neutrino scattering on nuclei during a supernova explosion and the accompanying nucleosynthesis [6].

The case studied in the present work is the reaction ^{58}Ni($\vec{p}, \vec{p}'$). The target ^{58}Ni has been investigated extensively in high-resolution electron scattering [7,8] and recently also in charge-exchange reactions [9,10] providing detailed information on low-multipolarity spin–isospin modes. The description of cross sections and spin–flip probabilities in the continuum from the present reaction is discussed elsewhere [11]. In this Letter we focus on cross sections and analyzing powers of elastic scattering and of the prominently excited levels up to 5 MeV excitation energy, serving as a benchmark for the models.

The optical model calculations are based on a microscopic description testing on the one hand different widely used parameterizations of the effective projectile–target interaction [12–14] and including on the other hand complex configurations such as two-particle two-hole (2p2h) states in the description of the wave functions of excited states. The nuclear structure input is based on the microscopic quasiparticle-phonon model (QPM) [15,16]. The DWBA calculations are performed with the code DWBA98 [17].

The ^{58}Ni($\vec{p}, \vec{p}'$) experiment was carried out at the KVI in Groningen, Netherlands. Unpolarized and transversely polarized protons with an energy of 172 MeV and currents varying between 1 and 4 nA were delivered by the superconducting cyclotron AGOR. The beam polarization was measured in regular time intervals with an in-beam polarimeter [18]. The average polarization of the beam was $65.6\% \pm 2.5\%$ for the spin-up state and $67.5\% \pm 2.5\%$ for the spin-down state of the polarized ion source. The outgoing protons were momentum analyzed by the Big-Bite spectrometer (BBS) [19] and detected with the EUROSUPERNOVA (ESN) system [20]. The ESN system is a focal-plane detector comprised of two vertical drift chambers and a focal-plane polarimeter consisting of a carbon analyzer and 4 multi-wire proportional chambers. Beam line and BBS were set up in dispersion-matched mode to ensure optimum energy

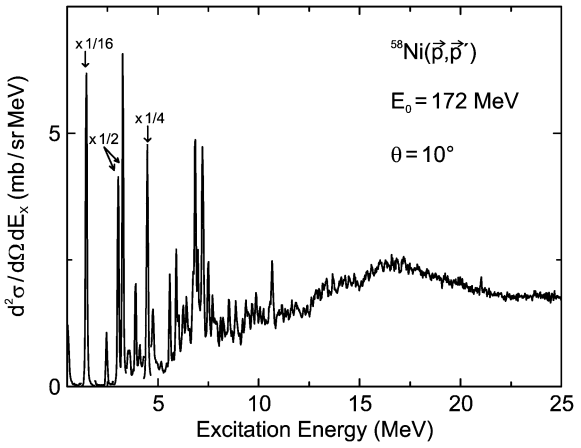

Fig. 1. Spectrum of the ^{58}Ni$(\vec{p},\vec{p}')$ reaction at $E_0 = 172$ MeV and $\theta = 10°$. The acquisition of elastically scattered protons was suppressed.

resolution. The spectrometer was placed at scattering angles $\theta = 4.5°$, 6°, 10° using a polarized beam and $\theta = 16°$, 19° with unpolarized beam. A self-supporting, 99% enriched ^{58}Ni foil with a thickness of 17.6 mg/cm^2 was used as target. Control measurements were performed with a ^{12}C target. Ref. [21] describes the data taking and analysis procedures of $(\vec{p},\vec{p}')$ experiments with the BBS-ESN setup.

A typical spectrum, taken at $\theta = 10°$, is shown in Fig. 1. In this case, the acquisition of elastically scattered protons was suppressed by the use of a veto scintillator in the focal plane detection system. The first line in the spectrum at $E_x = 1.45$ MeV excitation energy corresponds to the well-known 2_1^+ state in ^{58}Ni. The experimental energy resolution was $\Delta E \approx 80$ keV (FWHM). The strengths of this experiment compared to previous work are the possibility to measure cross sections and spin–flip observables at small scattering angles, the statistical significance of the data due to high data acquisition rates and the absence of instrumental background even at the most forward angles. Up to an excitation energy of 5 MeV, practically all experimentally observed levels can be matched with predictions of the QPM. This allows a one-to-one comparison between experiment and theory.

We start with a discussion of elastic scattering. In the upper part of Fig. 2 the angular distribution of the elastic scattering cross section and in the lower part that of the analyzing power are shown. Experimental data points of the present work are indicated by full tri-

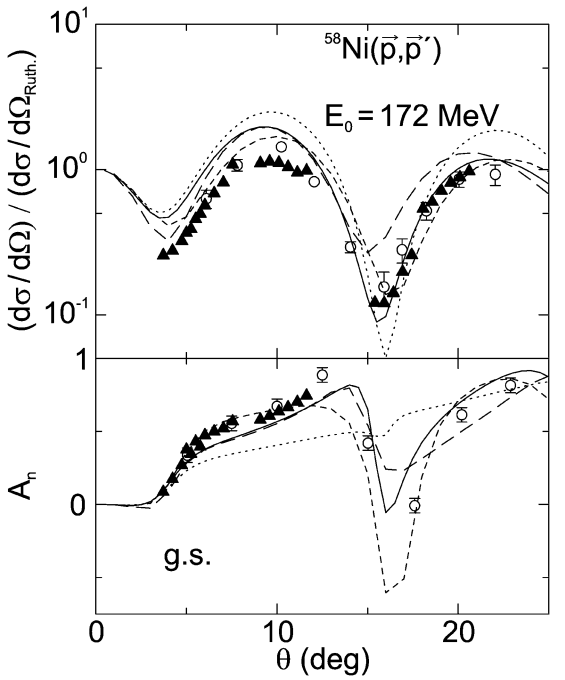

Fig. 2. Angular distributions of elastic scattering data. Upper part: cross section normalized to Rutherford cross section. Lower part: analyzing power. The full triangles represent data from the current experiment, the open circles are from an earlier experiment at $E_0 = 178$ MeV [22]. The solid, long-dashed, dotted and short-dashed lines correspond to calculations using models I–IV, respectively, described in the text.

angles. Data of an experiment using 178 MeV proton energy [22] are plotted as open circles. There is good agreement between the two data sets which rather precisely determine the second minimum around 16° in the angular distribution of the cross sections. The most forward-angle data extend almost exactly to the first minimum.

In a comparison to theoretical predictions elastic scattering serves primarily as a test of the reaction dynamics. Although the QPM is used here, the results exhibit little dependence on the particular model choice for the description of the ^{58}Ni ground state (g.s.) density distributions. A number of widely used effective projectile-target interactions are investigated in the following. These are G-matrix parameterizations of the Paris [12] (model I, solid lines) and the Bonn [13] (model II, long-dashed lines) potential, and the t-matrix parameterization of Love and Franey [14] (model III, dotted lines). The interactions are de-

fined by Yukawa functions in coordinate space. The g-matrix models use a density-dependent interaction. As a reference we add in Fig. 2 the results using the phenomenological optical model of Schwandt et al. [23] (model IV, short-dashed lines).

Large differences are observed among the model predictions for the cross sections as well as for the analyzing powers. Cross sections and analyzing powers are sensitive to different parts of the effective projectile–target interaction. For example, the spin–orbit interaction does not play an important role for cross sections but it is the dominant contribution for analyzing powers. Fig. 2 demonstrates that the microscopic optical models lead to a better overall description than the phenomenological one, except for the t-matrix parameterization which produces cross sections systematically a factor of two too high and fails for the analyzing power. The better agreement between the calculations with the G-matrix based interactions and data illustrates the importance of nuclear medium effects at this incident energy leading to density-dependent interactions. Nevertheless, all models have problems in reproducing the cross sections at the most forward angles. In the region of the first minimum around 4° as well as in the first maximum all calculations are systematically above the data. Here, the phenomenological model IV is actually doing best, but the second minimum and maximum are predicted at too small angles. Furthermore, the cross section in the second minimum is grossly overestimated while models I–III provide a good description.

In the next step, the ability of the microscopic optical model approach to describe collective low-energy transitions is investigated. A QPM calculation [16] provides excitation energies and wave functions of excited states from a diagonalization of the model Hamiltonian in a space of one- and two-phonon configurations. The QPM has been shown to account very well for the gross properties of collective modes and their fine structure at low [24–26] as well as high [8, 27] energies. The typical size of the model space is 1000–2000 configurations for each spin-parity value. The one-phonon components in the wave functions of the excited states were used as microscopic input into DWBA98 to calculate the corresponding transition densities and observables for each state. However, the inclusion of the two-phonon states is essential to obtain a realistic distribution of the one-phonon amplitudes due to configuration mixing.

Table 1
Excitation energies and transition strengths of collective states in ^{58}Ni (from [28]) compared to predictions of the QPM calculations described in the text

J^π	Exp.		QPM	
	E_x (MeV)	B(EJ) (e^2 fm^{2J})	E_x (MeV)	B(EJ) (e^2 fm^{2J})
2_1^+	1.45	648(27)	1.42	472
4_1^+	2.46	$1.70(12) \times 10^5$	2.69	1.07×10^5
2_2^+	3.04	67(6)	3.09	85
2_3^+	3.26	130(11)	3.24	100
3_1^-	4.47	$1.91(88) \times 10^4$	4.30	1.35×10^4
4_6^+	4.75	$3.31(25) \times 10^5$	$4.45 + 4.91$	4.18×10^4

There are two parameters of the QPM Hamiltonian which have to be determined by a fit to data. These are fixed by the requirement to optimally reproduce simultaneously the electromagnetic g.s. transition strength and excitation energies of the 2_1^+ and 3_1^- states, which represent the collective quadrupole and octupole vibration in ^{58}Ni, respectively. The model results for collective transitions below $E_x = 5$ MeV are summarized in Table 1. Comparison to the experimental data demonstrates a one-to-one correspondence except for the calculated 4^+ states at $E = 4.45$ MeV and 4.91 MeV, which are both close in energy to the experimental 4_6^+ state. The comparison is made for the sum of both. The assignment of transitions observed in the present experiment to known levels in ^{58}Ni [28] as indicated in Table 1 is also supported by the shapes of the cross section angular distributions characteristic for the transferred angular momentum.

In Fig. 3 the results for the collective quadrupole and octupole surface vibration in ^{58}Ni are shown in comparison to the various interaction model predictions. Model IV now corresponds to the phenomenological optical model to calculate the distortion while the interaction is that of model I. All effective interactions provide a good description of the angular distributions of the cross section. This is also true for the angular distributions of the analyzing power except, again, model III. The cross section magnitudes are very similar except for the use of the phenomenological optical model which leads systematically to about 30% larger values. More pronounced differences are

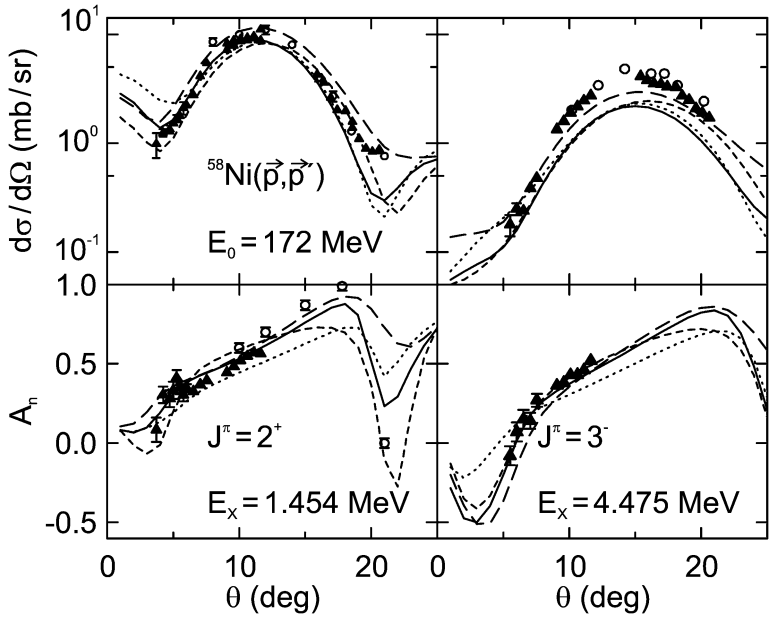

Fig. 3. Angular distributions of cross sections (upper part) and analyzing powers (lower part) for the 2_1^+ (left part) and 3_1^- (right part) states. Notations like in Fig. 2.

predicted at very small scattering angles $\theta \leqslant 3°$, experimentally still difficult to access. Note, that the theoretical predictions are absolute, i.e., no attempt has been made to normalize the calculations to the data.

The results for the other prominent transitions below $E_x = 5$ MeV excitation energy are displayed in Fig. 4. Calculations are shown for models I–III. Model IV is omitted here because, similar to the results in Fig. 3, the use of a phenomenological optical model does not improve the theoretical description. For the excitation of the 2^+ states at 3.04 and 3.26 MeV the cross sections are systematically too low because the collectivity of the transitions is underpredicted in the QPM (see Table 1). If the model results were normalized to the first maximum at $\theta \approx 12°$, the cross section angular distribution would be well reproduced for the transition to the $E_x = 3.04$ MeV state, but all calculations would slightly overshoot at small angles for the transition to the $E_x = 3.26$ MeV state. The angular distribution shapes are well reproduced for the excitations of the vibrational 4^+ states. Contrary to the cross sections calculated for the 2^+ states, which were very similar for all three interactions, model III predicts significantly larger values, while the results for models I and II are very close. The description of the analyzing powers is satisfactory with models I and II for all transitions and somewhat worse with model III.

The analysis of low-energy transitions in ^{58}Ni is based on the assumption that multistep contributions to the cross sections are negligible. This is certainly a good approximation for the collective quadrupole and octupole vibrations, but the QPM results suggest large two-phonon components in the wave functions of some of the transition shown in Fig. 4. For example, the first 4^+ state contains a 45% component of the $[2_1^+ \otimes 2_1^+; 4^+\rangle$ state and the $[2_1^+ \otimes 2_1^+; 2^+\rangle$ configuration is mixed with 42% and 18% into the 2^+ states at 2.69 and 3.24 MeV, respectively. At low incident proton energies, this may have a large impact on the description of the angular distributions requiring a full coupled-channel analysis [29,30]. However, at the incident energy of the present experiment coupled-channel effects should be small. For a rough estimate we have studied the role of multistep processes using the multistep direct reaction (MSDR) approach of Tamura, Udagawa and Lenske [31]. For a description of the current version of the model, see e.g. [32]. Applied to the present case, the overall contribution of two-step processes to the scattering cross sections is predicted to be less than one percent. Thus, even large two-phonon components in the wave functions can be

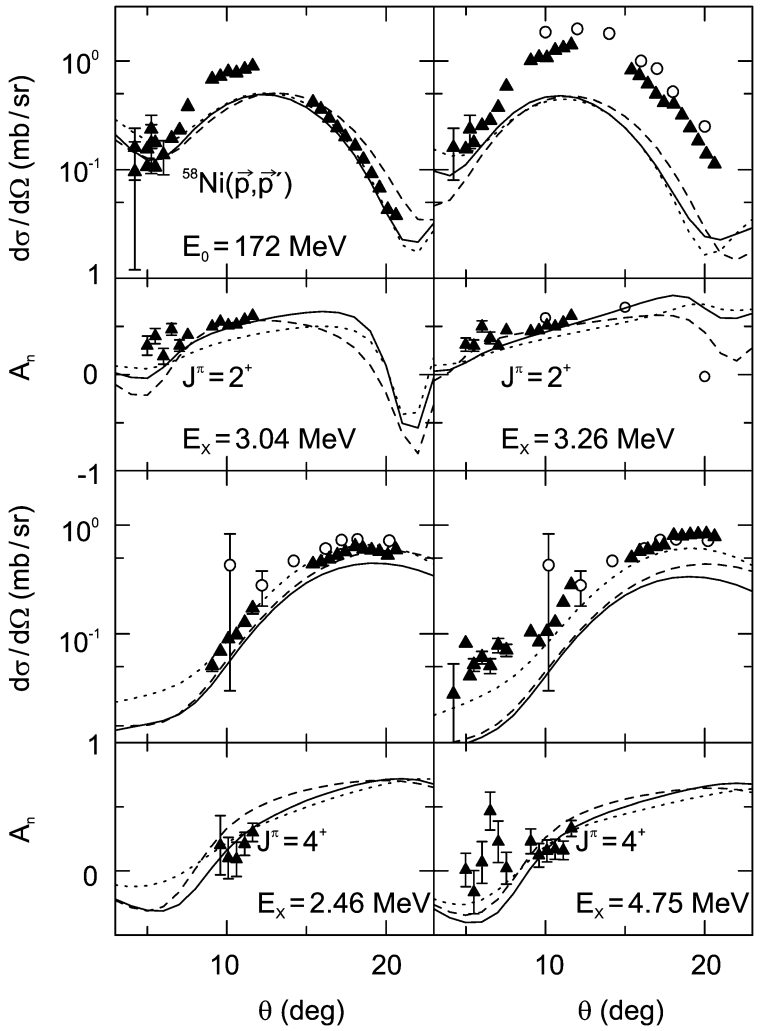

Fig. 4. Angular distributions of cross sections and analyzing powers for the 2_2^+, 2_3^+, 4_1^+ and 4_3^+ states. Notations for models I–III like in Fig. 2.

expected to contribute to the excitation cross sections on the level of a few percent only.

Finally, let us come back to the problems encountered when trying to reproduce the elastic scattering variables at small angles discussed above. In Fig. 5, we present a comparison with some alternative approaches. These are a G-matrix parameterization of the Paris potential in momentum space (model V, solid line) [33] and two results using relativistic Dirac models. The first one (model VI, short-dashed lines) uses the model of [34] with a projectile–target interaction based on the Paris potential. The other one (model VII, long-dashed lines) is performed within the simpler framework of relativistic impulse approximation, as discussed in [35], using again the Love–Franey t-matrix. The relativistic Love–Franey parameters at an incident energy of 170 MeV were extracted using the procedure described by Horowitz [36].

Model V gives a good overall description of cross sections and analyzing powers. The relativistic calculation VI is able to reproduce the cross section at very forward angles, but overshoots in the region of the first maximum like the nonrelativistic approaches. Furthermore, it fails for the analyzing power. How-

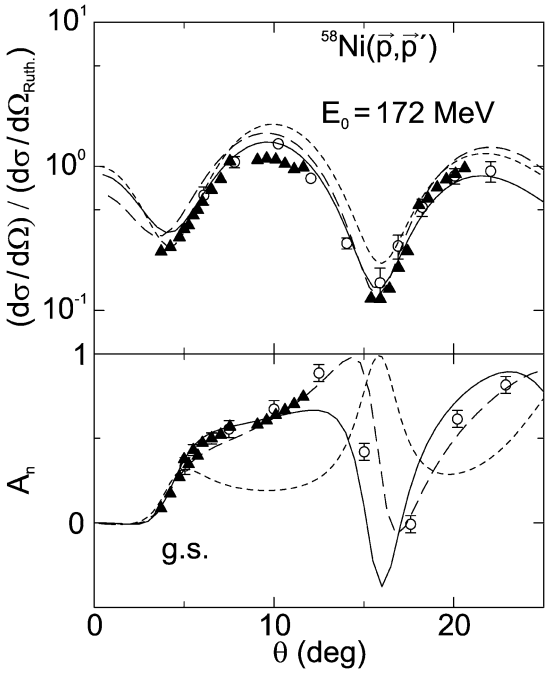

Fig. 5. Angular distributions of elastic scattering data (same as in Fig. 2) compared with model calculations V–VII, described in the text, using a G-matrix parameterization in momentum space (full lines) and a relativistic calculation (short-dashed lines), both based on the NN Paris potential, and a t-matrix in relativistic impulse approximation (long-dashed lines).

ever, it should be noted that the optical model of [34] is derived at much higher energies than applied in the present case. Finally, the results of model VII are comparable to those of V at small angles and for the analyzing power. The magnitude of the second maximum is slightly overestimated. The better agreement of calculations performed in momentum space compared to those performed in coordinate space may point to deficiencies in mapping the effective interactions from momentum to coordinate space.

In summary, we have presented cross sections and analyzing powers of the ^{58}Ni($\vec{p},\vec{p}'$) reaction at $E_0 = 172$ MeV and at forward angles, focusing on elastic scattering and prominent transitions at low excitation energy. They are used as a test case for the reliability of modern microscopic optical model approaches. Although the inelastic transitions are reasonably well described, the examination of elastic scattering at forward angles reveals surprising problems in the effective projectile–target interactions for both, nonrelativistic and relativistic models. Further investigations are necessary to discover the origin of this failure, keeping in mind the goal of extracting the properties of spin–isospin modes from (p, p') cross sections at very forward angles. Experimental programs aiming at the study of GT and SD resonances with inelastic proton scattering are under way at iThemba LABS, Somerset West, South Africa, and at KVI, respectively. A promising interaction for the description of elastic scattering is the one of model V, which uses a more refined G-matrix parameterization in momentum space. It would be interesting to extend this approach to the calculation of excited states.

Acknowledgements

We are indebted to H. Arrellano, H.W. von Geramb, G.C. Hillhouse, K. Kaki, S. Karataglidis and J. Raynal for enlightening discussions. We thank H. Arrellano and H.W. von Geramb for providing us with calculations of elastic scattering with models V and VI and G.C. Hillhouse for model calculation VII.

References

[1] K. Amos, et al., Adv. Nucl. Phys. 25 (2000) 275.
[2] D. Frekers, Nucl. Phys. A 731 (2004) 76.
[3] Y. Fujita, et al., Phys. Rev. Lett. 92 (2004) 062502.
[4] Y. Fujita, et al., Phys. Lett. B 365 (1996) 29.
[5] K. Langanke, G. Martínez-Pinedo, Rev. Mod. Phys. 75 (2003) 819.
[6] K. Langanke, G. Martínez-Pinedo, P. von Neumann-Cosel, A. Richter, Phys. Rev. Lett. 93 (2004) 202501.
[7] W. Mettner, et al., Nucl. Phys. A 473 (1987) 160.
[8] B. Reitz, et al., Phys. Lett. B 532 (2002) 179.
[9] Y. Fujita, et al., Eur. Phys. J. A 13 (2002) 411.
[10] M. Hagemann, et al., Phys. Lett. B 579 (2004) 251.
[11] F. Hofmann, et al., in preparation.
[12] H.V. von Geramb, in: H.O. Meyer (Ed.), Proceedings of International Conference Interactions Between Medium Energy Nucleons in Nuclei, in: AIP Conf. Proc., vol. 97, 1983, p. 44.
[13] S. Karataglidis, et al., Phys. Rev. C 52 (1995) 861.
[14] M.A. Franey, W.G. Love, Phys. Rev. C 31 (1985) 488.
[15] V.G. Soloviev, Theory of Atomic Nuclei, Quasiparticles and Phonons, IOP Publishing, Bristol, 1992.
[16] C.A. Bertulani, V.Yu. Ponomarev, Phys. Rep. 321 (1999) 139.
[17] J. Raynal, Computer code DWBA98, NEA Data Services NEA-1209/005.
[18] R. Bieber, et al., Nucl. Instrum. Methods A 457 (2001) 12.
[19] A.M. van den Berg, Nucl. Instrum. Methods B 99 (1995) 637.

[20] H.J. Wörtche, Nucl. Phys. A 687 (2001) 321c.
[21] V.M. Hannen, et al., Phys. Rev. C 67 (2003) 054320;
V.M. Hannen, et al., Phys. Rev. C 67 (2003) 054321.
[22] A. Ingemarsson, T. Johansson, G. Tibell, Nucl. Phys. A 365 (1981) 426.
[23] P. Schwandt, et al., Phys. Rev. C 26 (1982) 55.
[24] V.Yu. Ponomarev, P. von Neumann-Cosel, Phys. Rev. Lett. 82 (1999) 501.
[25] J. Enders, et al., Phys. Lett. B 486 (2000) 279;
J. Enders, et al., Nucl. Phys. A 724 (2003) 243.
[26] N. Ryezayeva, et al., Phys. Rev. Lett. 89 (2002) 272502.
[27] A. Shevchenko, et al., Phys. Rev. Lett. 93 (2004) 122501.
[28] M.R. Bhat, Nucl. Data Sheets 80 (1997) 789.
[29] H.P. Blok, et al., Nucl. Phys. A 386 (1982) 61.
[30] D.T. Khoa, I.N. Kuchtina, V.Yu. Ponomarev, Sov. J. Nucl. Phys. 44 (1986).
[31] T. Tamura, T. Udagawa, H. Lenske, Phys. Rev. C 26 (1982) 379.
[32] E. Ranström, H. Lenske, H.H. Wolter, Nucl. Phys. A 744 (2004) 108.
[33] H.F. Arellano, et al., Phys. Rev. C 54 (1996) 2570.
[34] A. Funk, H.V. von Geramb, K.A. Amos, Phys. Rev. C 64 (2001) 054003.
[35] D.P. Murdock, C.J. Horowitz, Phys. Rev. C 35 (1987) 1442.
[36] C.J. Horowitz, Phys. Rev. C 31 (1985) 1340.